HHS Public Access

Author manuscript

Circ Arrhythm Electrophysiol. Author manuscript; available in PMC 2024 September 01.

Published in final edited form as:

Circ Arrhythm Electrophysiol. 2023 September ; 16(9): e010891. doi:10.1161/CIRCEP.122.010891.

Sex and Gene Influence Arrhythmia Susceptibility in Murine Models of Calmodulinopathy

Lisa M. Wren, PhD[1], **Jean-Marc DeKeyser, MS**[1], **David Y. Barefield, PhD**[2], **Nicole A. Hawkins, PhD**[1], **Elizabeth M. McNally, MD, PhD**[3], **Jennifer A. Kearney, PhD**[1], **J. Andrew Wasserstrom, PhD**[4], **Alfred L. George Jr., MD**[1]

[1]Department of Pharmacology The Feinberg Cardiovascular and Renal Research Institute, Northwestern University Feinberg School of Medicine, Chicago;

[2]Department of Cell and Molecular Physiology, Loyola University Chicago, Maywood, IL

[3]Center for Genetic Medicine, The Feinberg Cardiovascular and Renal Research Institute, Northwestern University Feinberg School of Medicine, Chicago;

[4]Department of Medicine, The Feinberg Cardiovascular and Renal Research Institute, Northwestern University Feinberg School of Medicine, Chicago;

Abstract

Background -—Pathogenic variants in genes encoding calmodulin (CaM) are associated with a life-threatening ventricular arrhythmia syndrome (calmodulinopathy). The *in vivo* consequences of CaM variants have not been studied extensively and there is incomplete understanding of the genotype-phenotype relationship for recurrent variants. We investigated effects of different factors on calmodulinopathy phenotypes using two mouse models with a recurrent pathogenic variant (N98S) in *Calm1* or *Calm2*.

Methods -—Genetically engineered mice with heterozygous N98S pathogenic variants in *Calm1* or *Calm2* genes were generated. Differences between the sexes and affected gene were assessed using multiple physiological assays at the cellular and whole animal levels. Statistical significance among groups was evaluated using one-way analysis of variance (ANOVA) or the Kruskal-Wallis test when data were not normally distributed.

Results -—*Calm1*$^{N98S/+}$ (*Calm1*$^{S/+}$) or *Calm2* $^{N98S/+}$ (*Calm2*$^{S/+}$) mice exhibited sinus bradycardia and were more susceptible to arrhythmias after exposure to epinephrine and caffeine (epi/caf). Male *Calm1*$^{S/+}$ mice had the most severe arrhythmia phenotype with evidence of early embryonic lethality, greater susceptibility for arrhythmic events, frequent premature beats, QTc prolongation, and more heart rate variability after epi/caf than females with the same genotype. *Calm2*$^{S/+}$ mice exhibited a less severe phenotype, with female *Calm2*$^{S/+}$ mice having

Correspondence: Alfred L. George, Jr., MD, Department of Pharmacology, Northwestern University Feinberg School of Medicine, Searle 8-510, 320 East Superior Street, Chicago, IL 60611, Tel: 312-503-4893, al.george@northwestern.edu.

Disclosures: None

Supplemental Materials:
Supplemental Methods
Supplemental Tables S1–S17
Supplemental Figures S1–S5

the least severe arrhythmia susceptibility. Flecainide was not effective for preventing arrhythmias in heterozygous CaM-N98S mice. Intracellular Ca^{2+} transients observed in isolated ventricular cardiomyocytes from male heterozygous CaM-N98S mice had lower peak amplitudes and slower SR Ca^{2+} release following *in vitro* exposure to epi/caf, which were not observed in cardiomyocytes from heterozygous female CaM-N98S mice.

Conclusion -—We report heterogeneity in arrhythmia susceptibility and cardiomyocyte Ca^{2+} dynamics among male and female mice heterozygous for a recurrent pathogenic variant in *Calm1* or *Calm2*, illustrating a complex calmodulinopathy phenotype *in vivo*. Further investigation of sex and genetic differences may help identify the molecular basis for this heterogeneity.

Graphical Abstract

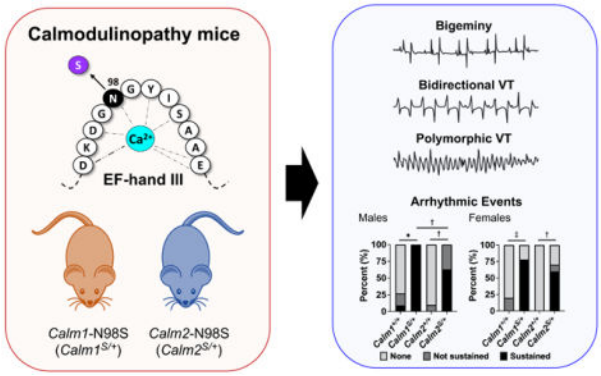

Keywords

arrhythmia; calmodulin; mouse model; Ca^{2+} dynamics; flecainide; CPVT

Introduction

Pathogenic variants in three distinct genes (*CALM1*, *CALM2*, *CALM3*) encoding the ubiquitous calcium (Ca^{2+}) sensor protein calmodulin (CaM) are associated with a life-threatening arrhythmia syndrome referred to as calmodulinopathy.[1–3] Common clinical features of calmodulinopathy include prolongation of the corrected QT (QTc) interval on an electrocardiogram (ECG) or stress-induced polymorphic ventricular tachycardia (PVT) associated with cardiac arrest and sudden cardiac death in infants and children.[4–8] While calmodulinopathy can resemble the clinical presentations of the congenital long-QT syndrome (LQTS) or catecholaminergic polymorphic ventricular tachycardiac (CPVT), there are also distinct aspects of this phenotype. In particular, the usual pharmacological strategies to minimize the risk of sudden cardiac death in LQTS and CPVT including β-adrenergic receptor antagonists, calcium channel and sodium channel blockers, appear less effective at mitigating sudden death risk in this condition.[5, 9, 10] A greater understanding of calmodulinopathy mechanisms may guide the identification of more effect therapeutic strategies.

CaM is ubiquitously expressed in human tissues and regulates the activity and function of various intracellular and plasma membrane proteins.[11, 12] Three genes (*CALM1*, *CALM2*,

or *CALM3*) encode identical CaM proteins consisting of 149 amino acid residues.[1, 13] CaM contains four Ca^{2+} binding EF-hand motifs, with EF-hands I and II being located in the N-terminal domain and EF-hands III and IV located within the C-terminal domain.[14] Mutations in EF-hands III and IV account for 80% of pathogenic CaM variants with the majority affecting residues that participate in binding Ca^{2+} ions.[10] Most pathogenic CaM variants cause impaired Ca^{2+} binding by the C-domain.[5, 6, 8, 15, 16] This reduced affinity leads to impaired Ca^{2+}-dependent inactivation (CDI) of L-type Ca^{2+} channels (LTCC) and prolonged action potentials (AP) in a variety of cellular models.[8, 15, 17, 18] By contrast, CaM variants associated with stress-induced PVT affect RyR2 function and promote abnormal sarcoplasmic reticulum (SR) Ca^{2+} release in ventricular cardiomyocytes leading to arrhythmogenic delayed after depolarizations (DADs), which increase the likelihood of ventricular arrhythmias and sudden death.[19–21] Some patients with calmodulinopathy display an overlap of arrhythmia phenotypes suggesting that multiple mechanisms may be involved.

The most frequent recurrent pathogenic CaM variant (N98S) was previously identified in *CALM1* and *CALM2* genes in association with distinct clinical phenotypes.[4, 6, 10, 22–24] At the protein level, *CALM1*-N98S and *CALM2*-N98S translate into identical CaM proteins. However, it is unclear what drives phenotypic heterogeneity in patients expressing this variant. Clinical data from N98S-positive patients report various differences in general characteristics such as sex, ethnicity, age and which CaM gene is expressing the pathogenic variant. Investigating the effects of these various factors in an *in vivo* calmodulinopathy model may reveal information about this complex genotype-phenotype relationship.

In this study, we investigated two mouse models of calmodulinopathy heterozygous for the recurrent N98S pathogenic variant in either *Calm1* or *Calm2* and compared phenotypes among male and female mice with these genotypes. The main goal of the study was to assess whether sex and CaM gene were associated with variable degrees of arrhythmia susceptibility.

Methods

All data, analytical methods, and study materials supporting this study are available from the corresponding author on reasonable request for purposes of reproducing the results or replicating the procedures.

Animal Care

Experiments on mice were approved by the Northwestern University Animal Care and Use Committee in accordance with the National Institutes of Health Guide for the Care and Use of Laboratory Animals. The ARRIVE (Animal Research: Reporting of *in vivo* Experiments) guidelines were used for planning and implementing experiments.[25] Numbers of animals used in each experiment are presented in Supplemental Tables.

Mice

Calm1$^{N98S/+}$ (abbreviated *Calm1*$^{S/+}$) and *Calm2*$^{N98S/+}$ (abbreviated *Calm2*$^{S/+}$) mice were generated in the Northwestern University Transgenic and Targeted Mutagenesis Core

Facility. Single stranded repair DNA oligonucleotide, guide RNA, and Cas9 mRNA were co-injected into single-cell stage C57BL/6J embryos (guide RNA and repair DNA sequences are provided in Supplemental Table S1). Asparagine-98 (N98) was modified to serine (S) with a single nucleotide change of codon 98 (*Calm1*, MGI:88251, c.293A>G, N98S; *Calm2*, MGI:103250, c.293A>G, N98S) for *Calm1* or *Calm2* in separate embryos. Mosaic founder mice were genotyped initially using Sanger sequencing of PCR amplicons generated using Q5® DNA polymerase (New England Biolabs, Ipswich, MA) and cloned into plasmid pCR4-Blunt (Invitrogen, Waltham, MA). Founders heterozygous for the N98S variant without other on-target edits, insertions or deletions were selected for breeding.

Male $Calm1^{S/+}$ or $Calm2^{S/+}$ mice were intercrossed with inbred female C57BL/6J mice (Stock #000664; Jackson Laboratories, Bar Harbor, ME) $Calm1^{+/+}$ (abbreviated WT1) and heterozygous $Calm1^{S/+}$ littermate mice, and wildtype $Calm2^{+/+}$ (abbreviated WT2) and heterozygous $Calm2^{S/+}$ littermate mice, respectively. First generation offspring derived from the mosaic founders were genotyped initially by Sanger sequencing of approximately 1 kb PCR amplicons centered on the pathogenic variant generated using Q5® polymerase. Subsequent genotyping was performed using allele-specific digital droplet PCR (ddPCR) validated on sequence-confirmed heterozygous genomic DNA. Primer sequences are provided in Supplemental Table S2 and PCR conditions in Supplemental Table S3. Mice were housed in a Specific Pathogen Free (SPF) barrier facility that maintained a 14:10 light:dark cycle. All mice had access to food and water *ad libitum*. For all experiments, male and female mice at 2–4 months of age were used.

Statistical Analyses

Comparisons between the observed ratios of WT to mutant littermates or embryos to the expected Mendelian ratios were analyzed using a chi-square test. Survival of mice in each group was analyzed using the Mantel-Cox long-rank test. For other measurements, simple comparisons between WT vs mutant littermates were made using Student's t-test. The Shapiro-Wilk test was used to test for normal distribution of each dataset. Multiple group comparisons were made using one-way ANOVA test followed by Tukey's post-hoc test for normally distributed data whereas a Kruskal-Wallis test followed by Dunn's post-hoc test was used for data that was not normally distributed, except when comparing between male and female groups in which a two-way ANOVA test was performed followed by Sidak's post-hoc test. A p-value less than 0.05 was considered statistically significant.

A complete description of the methods is provided in the Data Supplement.

Results

Generation and features of heterozygous $Calm1^{N98S/+}$ and $Calm2^{N98S/+}$ mice

We generated heterozygous $Calm1^{S/+}$ and $Calm2^{S/+}$ knock-in mice on the C57BL/6J (B6) background strain using CRISPR/Cas9 genome editing. Sanger sequencing verified successful introduction of the c.293A>G variant at codon 98 (Fig. 1A) resulting in replacement of the highly conserved asparagine (N) with serine (S, Fig. 1B). Extended sequencing of a ~1 kb region centered on the target site excluded aberrant genomic editing

events. *Calm1*$^{S/+}$ and *Calm2*$^{S/+}$ knock-in mice were backcrossed to inbred B6 mice for at least 5 generations before performing experiments.

To assess the effect of the pathogenic variant on CaM gene expression, we performed reverse transcriptase droplet digital PCR (RT-ddPCR) to quantify expression levels of *Calm1*, *Calm2*, and *Calm3* transcripts in whole heart. In both WT and mutant mouse hearts, *Calm1* was the most highly expressed CaM transcript, followed by *Calm2* and *Calm3*, respectively (Fig. 1C; Supplemental Table S4). There were no significant differences in CaM gene expression between WT and N98S littermate mice when including both sexes (Fig. 1C). Interestingly, males expressed higher levels of *Calm1*, *Calm2*, and *Calm3* compared to female mice (Supplemental Table S4). We also used RT-ddPCR coupled with allele-specific probes and found no evidence of allelic imbalance (median *Calm1* allele ratio 1.035 [95% confidence interval 1.02–1.07]; median *Calm2* allele ratio 0.995 [95% confidence interval 0.97–1.02]).

The CaM-N98S variant had no effects on survival of heterozygous mice, but fewer *Calm1*$^{S/+}$ mice were born than expected for Mendelian inheritance ($p = 0.011$; Fig. 1D). Male *Calm1*$^{S/+}$ mice were the primary drivers of this effect, with only 30% of male offspring born with the N98S variant (Fig. 1D; Supplemental Table S5). Analysis of embryos between E8 and E20 also showed fewer *Calm1*-N98S than WT mice (Supplemental Table S5; $p = 0.0008$) suggesting early embryonic lethality. Among *Calm2*$^{S/+}$ mice, females were born at higher-than-expected ratios, but this did not affect the overall expectancy of alleles among littermates and the observed ratios were consistent with expected Mendelian inheritance (Fig. 1D; Supplemental Table S5). Male *Calm1*$^{S/+}$mice were significantly smaller than WT male littermates at age 8–10 weeks (WT: 24.2 ± 0.4g, N98S: 22.3 ± 0.3g, p=0.0013), but there were no differences in weights between female *Calm1*$^{S/+}$and WT1 littermates, or between *Calm2*$^{S/+}$and WT2 littermates of either sex.

We performed echocardiography on *Calm1*$^{S/+}$and *Calm2*$^{S/+}$ mice to evaluate heart morphology and contractile function (Supplemental Fig. S1A). M-mode-derived data showed no differences in left ventricular internal diameter, posterior wall thickness, ejection fraction or fractional shortening in *Calm1*$^{S/+}$and *Calm2*$^{S/+}$ mice compared to WT littermates (Supplemental Fig. S1B,C; Supplemental Table S6). These results indicate that CaM-N98S mice have structurally normal hearts with normal contractile function.

CaM-N98S causes sinus bradycardia in mice

To determine the effects of the N98S variant on basal heart rhythms we performed ECG recordings on *Calm1*$^{S/+}$and *Calm2*$^{S/+}$ mice (Fig. 2A,B). In comparison to WT littermates, *Calm1*$^{S/+}$and *Calm2*$^{S/+}$ mice exhibited sinus rhythm with significantly slower beat rates in both male and female mice (Fig. 2C). Slower heart rate correlated with proportionally longer RR-intervals in CaM-N98S mice (Fig. 2D). Baseline QTc and QRS duration were not significantly different between WT and mutant littermates (Supplemental Table S7). We did not observe spontaneous ventricular arrhythmia. These results demonstrate that CaM-N98S induces sinus bradycardia in both male and female mice regardless of which of the two genes are affected.

Effects of genotype and sex on arrhythmia severity

Data from the International Calmodulin Registry (ICaMR) indicates that approximately 80% of arrhythmia phenotypes are triggered by exercise or emotional stress and that stress-induced PVT occurs in nearly 30% of the registry population (Table 1).[10] Because we did not observe spontaneous ventricular arrhythmia, we co-administered epinephrine (2 mg/kg, i.p.) and caffeine (120 mg/kg, i.p.) to groups of WT and heterozygous *Calm1*$^{S/+}$and *Calm2*$^{S/+}$ littermate mice to test for pharmacologically inducible arrhythmia. This pharmacological paradigm is used widely to provoke arrhythmia in various mouse models.[26–29] Epinephrine and caffeine (epi/caf) treatment of *Calm1*$^{S/+}$ and *Calm2*$^{S/+}$ mice induced a variety of arrhythmic events that were rarely observed in *Calm1*$^{+/+}$ and *Calm2*$^{+/+}$ mice (Fig. 3A). The most prevalent arrhythmias were bigeminy and bidirectional ventricular tachycardia (BVT, Fig. 3B). The occurrence of PVT with sudden cardiac death was infrequent in both *Calm1*$^{S/+}$ (n=2/11) and *Calm1*$^{+/+}$ (n=1/11) groups (Fig. 3B; Supplemental Table S8). We also recorded telemetric ECG in a small cohort of non-anesthetized mice to exclude confounding effects of general anesthesia used in surface ECG recordings (Supplemental Fig. S2A). Results from telemetry were similar to surface ECG recordings and demonstrated sinus bradycardia in *Calm1*$^{S/+}$ mice in both light (*Calm1*$^{+/+}$, 552 ± 14 bpm; N98S, 440 ± 15 bpm; $p = 0.0007$) and dark (*Calm1*$^{+/+}$, 640 ± 23 bpm; N98S, 567 ± 14 bpm; $p = 0.0211$) cycles (Supplemental Fig. S2B). Telemetry also revealed significantly enhanced susceptibility to sustained arrhythmic events after epi/caf treatment compared to *Calm1*$^{+/+}$ littermate mice (*Calm1*$^{+/+}$, 0/6, 0%; *Calm1*$^{S/+}$, 5/7, 72%; $p = 0.0291$; Supplemental Fig. S2C,D).

Calm1$^{S/+}$ and *Calm2*$^{S/+}$ mice had significantly more arrhythmic events after epi/caf exposure than *Calm1*$^{+/+}$ and *Calm2*$^{+/+}$ littermate mice of both sexes (Fig. 3C). Female *Calm1*$^{S/+}$ and *Calm2*$^{S/+}$ mice, 22% and 30% of mice, respectively, did not have arrhythmic events. By contrast, 100% of male *Calm1*-N98S and *Calm2*-N98S mice exhibited some form of arrhythmia. Male *Calm1*$^{S/+}$ had the greatest incidence of sustained arrhythmias with 11/11 mice (100%) exhibiting continuous PVCs, BVT, or PVT compared to 5/8 (63%) male *Calm2*$^{S/+}$ mice with sustained arrhythmic events (Fig. 3C; Supplemental Tables S8 and S9).

Because premature ventricular contractions (PVCs) are known triggers of PVT, we quantified PVC incidence after epi/caf. *Calm1*$^{S/+}$ mice of both sexes exhibited significantly more PVCs compared to *Calm1*$^{+/+}$ littermates (Fig. 3D). Nearly half of *Calm2*$^{S/+}$ male and female mice experienced PVCs compared to none of the *Calm2*$^{+/+}$ littermate mice (Fig. 3D; Supplemental Tables S10 and S11).

We next compared heart rate variability (HRV) as represented by Poincaré plots between N98S mice and WT littermates after epi/caf exposure (Fig. 4A,B). Male *Calm1*$^{S/+}$ mice exhibited greater HRV (quantified as the standard deviation of the R-R interval) compared to *Calm1*$^{+/+}$ littermates after epi/caf (Fig. 4C). Similarly, female *Calm1*$^{S/+}$ mice had greater HRV after epi/caf compared to *Calm1*$^{+/+}$ littermate mice (Fig. 4D), but HRV was not different between female *Calm2*$^{S/+}$ and *Calm2*$^{+/+}$ littermates (Fig. 4D; Supplemental Tables S10 and S11). Together, these data indicate that CaM-N98S mice generally have greater susceptibility to arrhythmic events after epi/caf, but *Calm1*$^{S/+}$ confers greater arrhythmogenicity than *Calm2*$^{S/+}$.

Induced QTc and QRS prolongation in *Calm1*-N98S male mice

Prolongation of the QT-interval has been documented in nearly half of calmodulinopathy cases.[10] Therefore, we assessed the effect of the pathogenic CaM-N98S variant on QTc interval and QRS duration before and after epi/caf (Fig. 5A). At baseline, the QTc interval and QRS duration between male and female WT and N98S littermate mice were not significantly different (Fig. 5B,C; Supplemental Table S11). By contrast, QTc and QRS were significantly prolonged after epi/caf in male *Calm1*$^{S/+}$ mice compared to male *Calm1*$^{+/+}$ littermates (Fig. 5B,C). These phenomena were not observed in male *Calm2*$^{S/+}$ mice, female *Calm1*$^{S/+}$ and female *Calm2*$^{S/+}$ mice (Supplemental Fig. S3A,B; Supplemental Table S11).

Flecainide does not prevent arrhythmia in CaM-N98S mice

Previous studies demonstrated that flecainide reduces arrhythmia susceptibility in mouse models of CPVT by inhibition of the ryanodine receptor.[30, 31] Therefore, we sought to investigate the efficacy of flecainide in CaM-N98S mice using a blinded cross-over design (Fig. 6A). *Calm1*$^{S/+}$ or *Calm2*$^{S/+}$ mice were randomized to receive either vehicle (DMSO in PBS, i.p.) or flecainide (20 mg/kg, i.p.) 30 minutes before epi/caf challenge, then experiments were repeated 7 days later with the same mice being placed in the other treatment group. This dose of flecainide was previously demonstrated to give a plasma concentration within the therapeutic range (2.5 ± 0.2 μM) following i.p. administration.[32] Flecainide administration was associated with significant QTc and QRS prolongation compared to vehicle before the administration of epi/caf in male and female N98S mice. This was also evident after epi/caf in female N98S mice (Fig. 6B,C; Supplemental Table S12). Only QRS prolongation was observed after epi/caf administration in male N98S mice (Fig. 6B,C; Supplemental Table S12). These ECG changes are consistent with known effects of flecainide on the heart and provide verification of drug effect in our experiments.[33]

We investigated the effect of flecainide on arrhythmia susceptibility in CaM-N98S mice after epi/caf administration (Fig. 7A). Treatment with flecainide 30 minutes prior to epi/caf did not reduce the incidence or frequency of arrhythmic events in male or female CaM-N98S mice (Fig. 7B; Supplemental Table S13). These data show that acute administration of flecainide was not effective in preventing pharmacologically-induced arrhythmias in N98S mice.

Calm1$^{N98S/+}$ and *Calm2*$^{N98S/+}$ cause altered intracellular Ca^{2+} dynamics

Previous studies suggested that arrhythmogenesis in calmodulinopathy involves dysregulation of the ryanodine receptor type 2 (RyR2) and abnormal intracellular Ca^{2+} handling.[19–21] We investigated the effect of CaM-N98S on Ca^{2+} cycling at two pacing frequencies (Fig. 8A; Supplemental Fig. S4; Supplemental Tables S14 and S15, 1 Hz, cycle length 1000 ms; Supplemental Table S16 and S17, 3.3 Hz, cycle length 300 ms). Exposure of acutely isolated ventricular cardiomyocytes to epi/caf caused significant increases in the peak amplitude of intracellular Ca^{2+} transients in all groups, but the effect was smaller in cardiomyocytes from male *Calm1*$^{S/+}$ and *Calm2*$^{S/+}$ mice compared to cells from male WT littermate mice at both pacing frequencies (Fig. 8B; Supplemental Tables S14 and S16). By contrast, there were no differences in peak Ca^{2+} transient amplitudes after epi/caf in

cardiomyocytes from female *Calm1*$^{S/+}$ and *Calm2*$^{S/+}$ mice paced at either 1 or 3.3 Hz compared to cells from WT littermates (Fig. S4A; Supplemental Tables S15 and S17).

The Ca^{2+} transient rise time (10% to 90% of peak) was significantly longer in cardiomyocytes from male *Calm1*$^{S/+}$ and *Calm2*$^{S/+}$ mice at baseline compared to cells from male WT littermate mice when paced at 1 Hz (Fig. 8C; Supplemental Table S14) but not at 3.3 Hz (Supplemental Table S16), and this difference was absent after epi/caf treatment (Fig. 8C). The rise time was not different in cells from female *Calm1*$^{S/+}$ and *Calm2*$^{S/+}$ mice compared to cells from female WT littermate mice at baseline or after epi/caf (Supplemental Fig. S4B; Supplemental Table S15 and S17). Exposure to epi/caf shortened rise times in all groups. The Ca^{2+} transient decay time (90% to 10% of peak) was not different in cardiomyocytes from male or female *Calm1*$^{S/+}$ and *Calm2*$^{S/+}$ mice compared to cells from WT sex-matched littermates (Fig. 8D; Supplemental Fig. S4C; Supplemental Tables S14–S17). Exposure to epi/caf shortened decay times in *Calm1*$^{S/+}$ groups similar to WT littermates. However, decay times were greater in *Calm2*$^{S/+}$ groups compared to WT littermates (Supplemental Fig. S4C). The transient duration at 50% recovery (TD_{50}) was significantly longer in *Calm2*$^{S/+}$ male and female groups compared to WT littermates, but not different in cardiomyocytes from *Calm1*$^{S/+}$ groups compared to WT littermates after epi/caf when paced at either frequency (Fig. 8E; (Supplemental Fig. S4D; Supplemental Tables S15 and S17). However, at a faster pacing rate of 3.3 Hz, the transient duration at 80% recovery (TD_{80}) was significantly longer in cells from male *Calm1*$^{S/+}$ mice compared to cells from male WT littermate mice (Supplemental Table S16). This phenomenon was not observed in cells from male *Calm2*$^{S/+}$ or female *Calm1*$^{S/+}$ mice (Supplemental Table S14–S17).

The percent of cells exhibiting spontaneous Ca^{2+} waves was not different between WT and CaM-N98S groups (Supplemental Fig. S5A,B). Similarly, the Ca^{2+} wave frequencies between cells from WT and CaM-N98S littermate mice were nearly identical (Supplemental Fig. S5C,D). At baseline, the majority of Ca^{2+} waves occurred after 1 Hz pacing (Supplemental Fig. S5E). By contrast, after epi/caf the majority of Ca^{2+} waves occurred following the pause after 3.3 Hz pacing (Supplemental Fig. S5E). Importantly, early aftertransients (EATs) and delayed aftertransients (DATs), which are proxies for arrhythmogenic early and delayed afterdepolarizations (EADs, DADs), respectively, were too rare to analyze.

Discussion

In this study, we investigated arrhythmia susceptibility in two calmodulinopathy mouse models in which the most recurrent human calmodulin pathogenic variant (CaM-N98S) was engineered in either the *Calm1* or *Calm2* genes. These mice mirror genotypes that are associated with diverse arrhythmia phenotypes in humans including prolonged QTc, stress-induced PVT, and sudden death (Table 1). The basis for the genotype-phenotype heterogeneity associated with CaM-N98S is unclear from clinical studies, which are challenging given the rare and often *de novo* nature of the variants. Therefore, we employed genetically engineered mice to determine if two specific factors (sex, CaM gene) can explain this phenomenon.

Phenotypic heterogeneity in calmodulinopathy

Most cases in the ICaMR have pathogenic variants in *CALM1*, followed by *CALM2* and least frequently *CALM3*.[10] Differences in sex, ethnicity, specific variant and which CaM gene is mutated may contribute to the phenotype heterogeneity observed in this registry cohort. Even among cases heterozygous for the recurrent pathogenic variant N98S, variability in the clinical presentation of arrhythmia susceptibility exists (Table 1). The first report of this variant occurred in a 4-year-old Iraqi female heterozygous for *de novo CALM1*-N98S who had cardiac arrest while running. Later, she was noted to have complex ventricular ectopy before and during treatment with a β1-adrenergic-receptor blocker and a second cardiac arrest at age 15 years.[4] The QTc was not prolonged in this case. The second reported case was that of a *de novo* heterozygous *CALM2*- N98S variant in a 5-year-old Japanese male who experienced episodes of dizziness and syncope while running.[6] Evaluation of his ECGs revealed baseline prolongation of the QTc interval, which worsened with epinephrine infusion. Treatment with propranolol and mexiletine did not prevent syncopal episodes. Based on these initial two cases, it was suspected that heterozygous N98S variant in *CALM1* would specifically cause stress-induced PVT, while the same variant in *CALM2* evokes QTc prolongation, although the influence of sex and genetic background could not be excluded. However, Jiménez-Jáimez et al. later reported two cases in which heterozygous *CALM2*-N98S was associated with distinct clinical phenotypes including a 7-year-old Spanish male with sinus bradycardia, exercise-induced arrhythmias and SCD, and a 4-year-old Moroccan female with stress-induced LQTS.[22] There is no predominant phenotype among ten persons heterozygous for either *CALM1*-N98S or *CALM2*-N98S reported by the International Calmodulinopathy registry[10] including six cases in the published literature (Table 1). Interestingly, this variant has not been reported to occur in *CALM3*.

Comparisons of our two CaM-N98S mouse models revealed that male $Calm1^{S/+}$ mice exhibited the most severe phenotype with lower birth rates, QTc and QRS prolongation after exposure to epinephrine and caffeine, along with the greatest incidence of PVCs and sustained arrhythmias when compared to female $Calm1^{S/+}$, and male and female $Calm2^{S/+}$ mice. The *Calm1* mRNA levels in heart are significantly higher than *Calm2*, and all CaM genes are expressed at significantly higher levels in male compared to female mice. Consistent with this notion, modulating CaM gene expression rescues cellular arrhythmia phenotypes in patient-derived induced pluripotent stem cell-derived cardiomyocytes (iPSC-CMs).[34, 35]

We observed significant differences in phenotype severity between male and female CaM-N98S mice that is reminiscent of the sexual dimorphism observed in other genetic and acquired heart rhythm disorders.[36–39] In humans, females have longer QTc intervals and are more susceptible to torsades de pointes in the setting of drug induced LQTS. By contrast, men account for the majority of SCD cases and predominate among cases of Brugada syndrome and short QT syndrome. Hormonal regulation of calcium and potassium channels after puberty may account for sex differences in QTc duration, but the precise mechanisms involved are incompletely understood.[40] Calmodulinopathy cases in the ICaMR are evenly distributed between the sexes, but symptomatic disease is most common in males.[10] In a

previously reported mouse model of calmodulinopathy expressing the *Calm1*-N98S variant, female mice exhibited significantly shorter QTc intervals, no QRS prolongation, and a lower incidence of BVT compared to male *Calm1*$^{S/+}$ mice, similar to our mouse models.[41] Further investigation of mechanisms responsible for sex-specific arrhythmia susceptibility could reveal novel therapeutic targets. We did not observe baseline prolongation of the QTc interval in our mouse models and different genetic backgrounds used in the prior study (Table 2) could account for this difference.[26, 30, 32, 41–43]

Comparison of calmodulinopathy with CPVT

Some cases of calmodulinopathy are classified as CPVT or are described as CPVT-like. CPVT is a severe arrhythmia syndrome characterized by ectopic beats, BVT and PVT triggered by physical or emotional stress that can progress to syncope and SCD.[44] Pathogenic variants in *RYR2* (encoding ryanodine receptor 2, RyR2) account for the majority of CPVT cases, followed by variants in calsequestrin (*CASQ2*) and triadin (*TRDN*).[45] Similar to typical CPVT, sinus bradycardia and syncope after physical or emotional stress are reported in calmodulinopathy, although BVT is rare.[10] Although calmodulinopathy can resemble CPVT in the initiation and presentation of arrhythmia, there are key clinical features that distinguish these two conditions. The median age-of-onset (6 years) of calmodulinopathy is earlier than typical CPVT (10 years).[10, 46] In addition, CPVT is accompanied by normal QTc duration before and after adrenergic stimulation,[45] whereas calmodulinopathy is frequently associated with QTc prolongation including some cases with the pathogenic CaM-N98S variant.[6, 22] Therapy with β-adrenergic blockers is highly effective in preventing adrenergic-triggered arrhythmias in CPVT, but has inconsistent benefit in calmodulinopathy.[9, 10] Similarly, flecainide is effective in reducing arrhythmia risk in CPVT,[30, 47] but efficacy is less apparent in calmodulinopathy.[10] These phenotype distinctions are recapitulated in mouse models of both disorders.

There are also mechanistic distinctions between CPVT and calmodulinopathy (Table 2). In mouse models of CPVT, impaired function or regulation of RyR2 disrupts intracellular Ca^{2+} handling, leading to ectopic SR Ca^{2+} release and triggered arrhythmogenic DADs.[42, 48, 49] We did not observe DATs or EATs in *Calm1*$^{S/+}$ or *Calm2*$^{S/+}$ mice before or after exposure to epi/caf. Tsai et al. showed that DADs were not observed in *Calm1*$^{S/+}$ mice until mutant ventricular cardiomyocytes were paced at 7 Hz.[41] In our experimental set up, pacing rates greater than 3.3 Hz did not consistently capture ventricular beats and therefore we could not reliably assess Ca^{2+} transients at higher frequencies. Previous reports also suggest that impaired Ca^{2+} homeostasis of the Purkinje network, not necessarily the ventricular myocardium, trigger arrhythmogenic DADs and ectopic firing,[50, 51] but a recent study suggests that arrhythmia originates at the Purkinje-myocardial interface in CPVT.[52] Tsai et al. demonstrated by voltage mapping studies in their *Calm1*$^{S/+}$ mouse model that EADs detected within the His-Purkinje network after adrenergic stimulation may serve as the origin of arrhythmogenesis in the N98S calmodulinopathy model.[41] We did not assess Ca^{2+} dynamics of the conduction system in our mouse models.

A prominent feature of Ca^{2+} dynamics that we observed in cardiomyocytes isolated from *Calm1*$^{S/+}$ and *Calm2*$^{S/+}$ mice was lower Ca^{2+} peak amplitude and slower SR Ca^{2+}

release rate. Similarly, Tsai et al. reported significantly lower Ca^{2+} spark amplitudes and prolongation of time to peak after adrenergic stimulation compared to WT mice.[41] *In vitro* studies also revealed that the CaM-N98S variant increases the single-channel open probability of RyR2, resulting in a greater Ca^{2+} spark frequency and lower SR Ca^{2+} load.[19] In our study, we did not observe enhanced triggered activity in mutant mice. Together, these data suggest that CaM-N98S may promote RyR2 leakiness and reduces SR Ca^{2+} stores, and these effects likely contribute to arrhythmia susceptibility, but may not fully explain the calmodulinopathy phenotype. Further evidence that RyR2 dysregulation is not the sole mechanism underlying arrhythmogenicity is our data demonstrating lack of antiarrhythmic efficacy for flecainide in CaM-N98S mice.

In addition to impaired Ca^{2+} homeostasis, other mechanisms of arrhythmogenesis have been proposed in CaM-N98S mice. Tsai et al. reported impaired inactivation of LTCC and the prolongation of action potentials after adrenergic stimulation.[41] This is a primary mechanism of QTc prolongation that may potentiate the risk of arrhythmia susceptibility. Therefore, we suspect that the prolongation of the QTc interval in our male *Calm1*$^{S/+}$ mice may be a result of similar mechanisms of LTCC dysregulation and impaired CDI. Because QTc prolongation was not present at baseline in our mouse models, we did not investigate the effect of CaM-N98S on sarcolemmal ion channel function.

Study limitations

While our study offers unique insights into factors that influence arrhythmia predisposition in calmodulinopathy, other studies are required to elucidate the exact molecular basis for the gene and sex dependence of the phenotype we observed. As discussed above, we did not observe QTc prolongation at baseline in our two new mouse models even though this is a documented feature of some CaM-N98S carriers (Table 1). Repolarization in mouse heart is distinct from human heart and a murine model of calmodulinopathy may be suboptimal to replicate this feature of the clinical phenotype. Because there were multiple tests of significance from multiple comparisons, our study has an increased chance of false positive correlations. Finally, given the partial embryonic lethality of the calmodulin mutation, our study may be confounded by ascertainment bias.

Conclusions

We report investigations of two murine models of calmodulinopathy caused by the recurrent N98S pathogenic variant expressed in two different CaM genes. We observed greater arrhythmia susceptibility in male and *Calm1*$^{S/+}$ mice indicating that sex and CaM gene are trait modifiers. We also highlight a pattern of abnormal Ca^{2+} dynamics in calmodulinopathic cardiomyocytes that differ from models of CPVT, and demonstrate that flecainide lacks antiarrhythmic efficacy in calmodulinopathy. Our findings illustrate the complex arrhythmia mechanisms in calmodulinopathy and identify factors that contribute to phenotypic heterogeneity in this disorder.

Supplementary Material

Refer to Web version on PubMed Central for supplementary material.

Sources of Funding:

This work was supported by NIH grants HL083374 and HL122010 (A.L.G.), and a predoctoral fellowship from the American Heart Association (L.M.W.).

Nonstandard Abbreviations and Acronyms

BVT	bidirectional ventricular tachycardia
CaM	calmodulin protein
Calm1 $^{S/+}$	notation for mice heterozygous for Calm1-N98S variant
Calm2 $^{S/+}$	notation for mice heterozygous for Calm2-N98S variant
Calm1 $^{+/+}$	notation for wildtype *Calm1* mice
Calm2 $^{+/+}$	notation for wildtype *Calm2* mice
CPVT	catecholaminergic polymorphic ventricular tachycardia
ddPCR	digital droplet polymerase chain reaction
DAD	delayed afterdepolarizations
DAT	delayed aftertransients
EAD	early afterdepolarizations
EAT	early aftertransients
epi	epinephrine infusion test
epi/caf	epinephrine and caffeine
HR	heart rate
HRV	heart rate variability
ICaMR	International Calmodulinopathy Registry
ICD	implantable cardioverter defibrillator
LQT	long-QT
LTCC	L-type calcium channel
PVC	premature ventricular contraction
PVT	polymorphic ventricular tachycardia
RT	reverse transcription
RYR	ryanodine receptor
SCA	sudden cardiac arrest

SCD	sudden cardiac death
TdP	torsades de pointes
VF	ventricular fibrillation
VT	ventricular tachycardia

References:

1. Fischer R, Koller M, Flura M, Mathews S, Strehler-Page MA, Krebs J, Penniston JT, Carafoli E, Strehler EE. Multiple divergent mRNAs code for a single human calmodulin. J Biol Chem. 1988;263:17055–17062. [PubMed: 3182832]
2. George AL Jr. Calmodulinopathy: a genetic trilogy. Heart Rhythm. 2015;12:423–4. [PubMed: 25460856]
3. Kotta MC, Sala L, Ghidoni A, Badone B, Ronchi C, Parati G, Zaza A, Crotti L. Calmodulinopathy: A novel, life-threatening clinical entity affecting the young. Front Cardiovasc Med. 2018;5:175. [PubMed: 30574507]
4. Nyegaard M, Overgaard MT, Sondergaard MT, Vranas M, Behr ER, Hildebrandt LL, Lund J, Hedley PL, Camm AJ, Wettrell G, et al. Mutations in calmodulin cause ventricular tachycardia and sudden cardiac death. Am J Hum Genet. 2012;91:703–712. [PubMed: 23040497]
5. Crotti L, Johnson CN, Graf E, De Ferrari GM, Cuneo BF, Ovadia M, Papagiannis J, Feldkamp MD, Rathi SG, Kunic JD, et al. Calmodulin mutations associated with recurrent cardiac arrest in infants. Circulation. 2013;127:1009–1017. [PubMed: 23388215]
6. Makita N, Yagihara N, Crotti L, Johnson CN, Beckmann BM, Roh MS, Shigemizu D, Lichtner P, Ishikawa T, Aiba T, et al. Novel calmodulin mutations associated with congenital arrhythmia susceptibility. Circ Cardiovasc Genet. 2014;7:466–474. [PubMed: 24917665]
7. Marsman RF, Barc J, Beekman L, Alders M, Dooijes D, van den WA, Ratbi I, Sefiani A, Bhuiyan ZA, Wilde AA, et al. A mutation in CALM1 encoding calmodulin in familial idiopathic ventricular fibrillation in childhood and adolescence. J Am Coll Cardiol. 2014;63:259–266. [PubMed: 24076290]
8. Wren LM, Jiménez-Jáimez J, Al-Ghamdi S, Al-Aama JY, Bdeir A, Al-Hassnan ZN, Kuan JL, Foo RY, Potet F, Johnson CN, et al. Genetic mosaicism in calmodulinopathy. Circ Genom Precis Med. 2019;12:375–385. [PubMed: 31454269]
9. Webster G, Schoppen ZJ, George AL Jr. Treatment of calmodulinopathy with verapamil. BMJ Case Rep. 2017;2017.
10. Crotti L, Spazzolini C, Tester DJ, Ghidoni A, Baruteau AE, Beckmann BM, Behr ER, Bennett JS, Bezzina CR, Bhuiyan ZA, et al. Calmodulin mutations and life-threatening cardiac arrhythmias: insights from the International Calmodulinopathy Registry. Eur Heart J. 2019;40:2964–2975. [PubMed: 31170290]
11. Uhlén M, Fagerberg L, Hallström BM, Lindskog C, Oksvold P, Mardinoglu A, Sivertsson Å, Kampf C, Sjöstedt E, Asplund A, et al. Proteomics. Tissue-based map of the human proteome. Science. 2015;347:1260419.
12. Clapham DE. Calcium signaling. Cell. 2007;131:1047–58. [PubMed: 18083096]
13. Toutenhoofd SL, Foletti D, Wicki R, Rhyner JA, Garcia F, Tolon R, Strehler EE. Characterization of the human CALM2 calmodulin gene and comparison of the transcriptional activity of CALM1, CALM2 and CALM3. Cell Calcium. 1998;23:323–38. [PubMed: 9681195]
14. Sorensen AB, Søndergaard MT, Overgaard MT. Calmodulin in a heartbeat. FEBS J. 2013;280:5511–32. [PubMed: 23663249]
15. Boczek NJ, Gomez-Hurtado N, Ye D, Calvert ML, Tester DJ, Kryshtal D, Hwang HS, Johnson CN, Chazin WJ, Loporcaro CG, et al. Spectrum and Prevalence of CALM1-, CALM2-, and CALM3-Encoded Calmodulin (CaM) Variants in Long QT Syndrome (LQTS) and Functional Characterization of a Novel LQTS-Associated CaM Missense Variant, E141G. Circ Cardiovasc Genet. 2016;9:136–146. [PubMed: 26969752]

16. Pipilas DC, Johnson CN, Webster G, Schlaepfer J, Fellmann F, Sekarski N, Wren LM, Ogorodnik KV, Chazin DM, Chazin WJ, et al. Novel calmodulin mutations associated with congenital long QT syndrome affect calcium current in human cardiomyocytes. Heart Rhythm. 2016;13:2012–2019. [PubMed: 27374306]
17. Limpitikul WB, Dick IE, Joshi-Mukherjee R, Overgaard MT, George AL, Yue DT Jr.. Calmodulin mutations associated with long QT syndrome prevent inactivation of cardiac L-type Ca currents and promote proarrhythmic behavior in ventricular myocytes. J Mol Cell Cardiol. 2014;74:115–124. [PubMed: 24816216]
18. Yin G, Hassan F, Haroun AR, Murphy LL, Crotti L, Schwartz PJ, George AL, Satin J. Arrhythmogenic calmodulin mutations disrupt intracellular cardiomyocyte Ca^{2+} regulation by distinct mechanisms. J Am Heart Assoc. 2014;3:e000996.
19. Hwang HS, Nitu FR, Yang Y, Walweel K, Pereira L, Johnson CN, Faggioni M, Chazin WJ, Laver DR, George A Jr., et al. Divergent regulation of RyR2 calcium release channels by arrhythmogenic human calmodulin missense mutants. Circ Res. 2014;114:1114–1124. [PubMed: 24563457]
20. Sondergaard MT, Tian X, Liu Y, Wang R, Chazin WJ, Chen SR, Overgaard MT. Arrhythmogenic calmodulin mutations affect the activation and termination of cardiac ryanodine receptor-mediated Ca^{2+} release. J Biol Chem. 2015;290:26151–26162. [PubMed: 26309258]
21. Gomez-Hurtado N, Boczek NJ, Kryshtal DO, Johnson CN, Sun J, Nitu FR, Cornea RL, Chazin WJ, Calvert ML, Tester DJ, et al. Novel CPVT-associated calmodulin mutation in CALM3 (CALM3-A103V) activates arrhythmogenic Ca waves and sparks. Circ Arrhythm Electrophysiol 2016;9:e004161. [PubMed: 27516456]
22. Jiménez-Jáimez J, Palomino Doza J, Ortega Á, Macías-Ruiz R, Perin F, Rodríguez-Vázquez del Rey MM, Ortiz-Genga M, Monserrat L, Barriales-Villa R, Blanca E, et al. Calmodulin 2 Mutation N98S Is Associated with Unexplained Cardiac Arrest in Infants Due to Low Clinical Penetrance Electrical Disorders. PLoS One. 2016;11:e0153851.
23. Daly A, Johnson NM, Decker E, Callis TE, Tahiliani J, Garcia J, Aguilar S, Murillo L, Herrera B, Beltran D, et al. Pathogenic variants in calmodulin associated with resuscitated childhood cardiac arrest. Heart Rhythm. 2017;14:S2.
24. Fujita S, Nakagawa R, Futatani T, Igarashi N, Fuchigami T, Saito S, Ohno S, Horie M, Hatasaki K. Long QT syndrome with a de novo CALM2 mutation in a 4-year-old boy. Pediatr Int. 2019;61:852–858. [PubMed: 31283864]
25. Percie du Sert N, Hurst V, Ahluwalia A, Alam S, Avey MT, Baker M, Browne WJ, Clark A, Cuthill IC, Dirnagl U, et al. The ARRIVE guidelines 2.0: Updated guidelines for reporting animal research. Br J Pharmacol. 2020;177:3617–3624. [PubMed: 32662519]
26. Liu N, Colombi B, Memmi M, Zissimopoulos S, Rizzi N, Negri S, Imbriani M, Napolitano C, Lai FA, Priori SG. Arrhythmogenesis in catecholaminergic polymorphic ventricular tachycardia: insights from a RyR2 R4496C knock-in mouse model. Circ Res. 2006;99:292–298. [PubMed: 16825580]
27. Mathur N, Sood S, Wang S, van Oort RJ, Sarma S, Li N, Skapura DG, Bayle JH, Valderrabano M, Wehrens XH. Sudden infant death syndrome in mice with an inherited mutation in RyR2. Circ Arrhythm Electrophysiol. 2009;2:677–685. [PubMed: 20009080]
28. van Oort RJ, McCauley MD, Dixit SS, Pereira L, Yang Y, Respress JL, Wang Q, De Almeida AC, Skapura DG, Anderson ME, et al. Ryanodine receptor phosphorylation by calcium/calmodulin-dependent protein kinase II promotes life-threatening ventricular arrhythmias in mice with heart failure. Circulation. 2010;122:2669–79. [PubMed: 21098440]
29. Kato T, Yamamoto T, Nakamura Y, Nanno T, Fukui G, Sufu Y, Hamada Y, Maeda T, Nishimura S, Ishiguchi H, et al. Correction of impaired calmodulin binding to RyR2 as a novel therapy for lethal arrhythmia in the pressure-overloaded heart failure. Heart Rhythm. 2017;14:120–127. [PubMed: 27771553]
30. Watanabe H, Chopra N, Laver D, Hwang HS, Davies SS, Roach DE, Duff HJ, Roden DM, Wilde AA, Knollmann BC. Flecainide prevents catecholaminergic polymorphic ventricular tachycardia in mice and humans. Nat Med. 2009;15:380–383. [PubMed: 19330009]
31. Kryshtal DO, Blackwell DJ, Egly CL, Smith AN, Batiste SM, Johnston JN, Laver DR, Knollmann BC. RYR2 channel inhibition is the principal mechanism of flecainide action in CPVT. Circ Res. 2021;128:321–331. [PubMed: 33297863]

32. Liu N, Denegri M, Ruan Y, Avelino-Cruz JE, Perissi A, Negri S, Napolitano C, Coetzee WA, Boyden PA, Priori SG. Short communication: flecainide exerts an antiarrhythmic effect in a mouse model of catecholaminergic polymorphic ventricular tachycardia by increasing the threshold for triggered activity. Circ Res. 2011;109:291–5. [PubMed: 21680895]
33. Heath BM, Cui Y, Worton S, Lawton B, Ward G, Ballini E, Doe CP, Ellis C, Patel BA, McMahon NC. Translation of flecainide- and mexiletine-induced cardiac sodium channel inhibition and ventricular conduction slowing from nonclinical models to clinical. J Pharmacol Toxicol Methods. 2011;63:258–68. [PubMed: 21194571]
34. Limpitikul WB, Dick IE, Tester DJ, Boczek NJ, Limphong P, Yang W, Choi MH, Babich J, DiSilvestre D, Kanter RJ, et al. A precision medicine approach to the rescue of function on malignant calmodulinopathic long-QT syndrome. Circ Res. 2017;120:39–48. [PubMed: 27765793]
35. Yamamoto Y, Makiyama T, Harita T, Sasaki K, Wuriyanghai Y, Hayano M, Nishiuchi S, Kohjitani H, Hirose S, Chen J, et al. Allele-specific ablation rescues electrophysiological abnormalities in a human iPS cell model of long-QT syndrome with a CALM2 mutation. Hum Mol Genet. 2017;26:1670–1677. [PubMed: 28335032]
36. Kannankeril P, Roden DM, Darbar D. Drug-induced long QT syndrome. Pharmacol Rev. 2010;62:760–781. [PubMed: 21079043]
37. Tadros R, Ton AT, Fiset C, Nattel S. Sex differences in cardiac electrophysiology and clinical arrhythmias: epidemiology, therapeutics, and mechanisms. Can J Cardiol. 2014;30:783–92. [PubMed: 24970790]
38. Vink AS, Clur SB, Wilde AAM, Blom NA. Effect of age and gender on the QTc-interval in healthy individuals and patients with long-QT syndrome. Trends Cardiovasc Med. 2018;28:64–75. [PubMed: 28869094]
39. Asatryan B, Yee L, Ben-Haim Y, Dobner S, Servatius H, Roten L, Tanner H, Crotti L, Skinner JR, Remme CA, et al. Sex-related differences in cardiac channelopathies: Implications for clinical practice. Circulation. 2021;143:739–752. [PubMed: 33587657]
40. Kurokawa J, Kodama M, Clancy CE, Furukawa T. Sex hormonal regulation of cardiac ion channels in drug-induced QT syndromes. Pharmacol Ther. 2016;168:23–28. [PubMed: 27595633]
41. Tsai WC, Guo S, Olaopa MA, Field LJ, Yang J, Shen C, Chang CP, Chen PS, Rubart M. Complex arrhythmia syndrome in a knock-In mouse model carrier of the N98S Calm1 mutation. Circulation. 2020;142:1937–1955. [PubMed: 32929985]
42. Kannankeril PJ, Mitchell BM, Goonasekera SA, Chelu MG, Zhang W, Sood S, Kearney DL, Danila CI, De Biasi M, Wehrens XH, et al. Mice with the R176Q cardiac ryanodine receptor mutation exhibit catecholamine-induced ventricular tachycardia and cardiomyopathy. Proc Natl Acad Sci U S A. 2006;103:12179–84. [PubMed: 16873551]
43. Knollmann BC, Chopra N, Hlaing T, Akin B, Yang T, Ettensohn K, Knollmann BE, Horton KD, Weissman NJ, Holinstat I, et al. Casq2 deletion causes sarcoplasmic reticulum volume increase, premature Ca^{2+} release, and catecholaminergic polymorphic ventricular tachycardia. J Clin Invest. 2006;116:2510–2520. [PubMed: 16932808]
44. Leenhardt A, Denjoy I, Guicheney P. Catecholaminergic polymorphic ventricular tachycardia. Circ Arrhythm Electrophysiol. 2012;5:1044–52. [PubMed: 23022705]
45. Priori SG, Napolitano C, Memmi M, Colombi B, Drago F, Gasparini M, DeSimone L, Coltorti F, Bloise R, Keegan R, et al. Clinical and molecular characterization of patients with catecholaminergic polymorphic ventricular tachycardia. Circulation. 2002;106:69–74. [PubMed: 12093772]
46. Kallas D, Lamba A, Roston TM, Arslanova A, Franciosi S, Tibbits GF, Sanatani S. Pediatric catecholaminergic polymorphic ventricular tachycardia: A translational perspective for the clinician-scientist. Int J Mol Sci. 2021;22:9293. [PubMed: 34502196]
47. Kannankeril PJ, Moore JP, Cerrone M, Priori SG, Kertesz NJ, Ro PS, Batra AS, Kaufman ES, Fairbrother DL, Saarel EV, et al. Efficacy of flecainide in the treatment of catecholaminergic polymorphic ventricular tachycardia: A randomized clinical trial. JAMA Cardiol. 2017;2:759–766. [PubMed: 28492868]

48. Liu N, Colombi B, Memmi M, Zissimopoulos S, Rizzi N, Negri S, Imbriani M, Napolitano C, Lai FA, Priori SG. Arrhythmogenesis in catecholaminergic polymorphic ventricular tachycardia: insights from a RyR2 R4496C knock-in mouse model. Circ Res. 2006;99:292–8. [PubMed: 16825580]

49. Wleklinski MJ, Kannankeril PJ, Knollmann BC. Molecular and tissue mechanisms of catecholaminergic polymorphic ventricular tachycardia. J Physiol. 2020;598:2817–2834. [PubMed: 32115705]

50. Cerrone M, Noujaim SF, Tolkacheva EG, Talkachou A, O'Connell R, Berenfeld O, Anumonwo J, Pandit SV, Vikstrom K, Napolitano C, et al. Arrhythmogenic mechanisms in a mouse model of catecholaminergic polymorphic ventricular tachycardia. Circ Res. 2007;101:1039–48. [PubMed: 17872467]

51. Herron TJ, Milstein ML, Anumonwo J, Priori SG, Jalife J. Purkinje cell calcium dysregulation is the cellular mechanism that underlies catecholaminergic polymorphic ventricular tachycardia. Heart Rhythm. 2010;7:1122–8. [PubMed: 20538074]

52. Blackwell DJ, Faggioni M, Wleklinski MJ, Gomez-Hurtado N, Venkataraman R, Gibbs CE, Baoudenbacher FJ, Gong S, Fishman GI, Boyle PM, et al. The Purkinje-myocardial junction is the anatomical origin of ventricular arrhythmia in CVPT. JCI Insight. 2022;7:e151893.

What is Known:

- Calmodulin transduces intracellular Ca2+ into signaling events involved with myriad physiological processes including cardiomyocyte excitation and contraction.
- Pathogenic variants in three human genes encoding identical calmodulin proteins are associated with a life-threatening cardiac arrhythmia syndrome called calmodulinopathy.
- The most recurrent pathogenic variant (conversion of asparagine-98 to serine, N98S) arises in two calmodulin genes (CALM1, CALM2) and is associated with diverse clinical arrhythmia phenotypes.

What the Study Adds:

- Genetically engineered mice heterozygous for Calm1-N98S or Calm2-N98S exhibit catecholamine-inducible ventricular arrhythmia.
- Arrhythmia susceptibility is most severe in male Calm1-N98S mice and least severe in female Calm2-N98S mice. Male Calm1-N98S mice exhibit embryonic lethality.
- Flecainide was ineffective at preventing induced ventricular arrhythmias in calmodulinopathic mice.

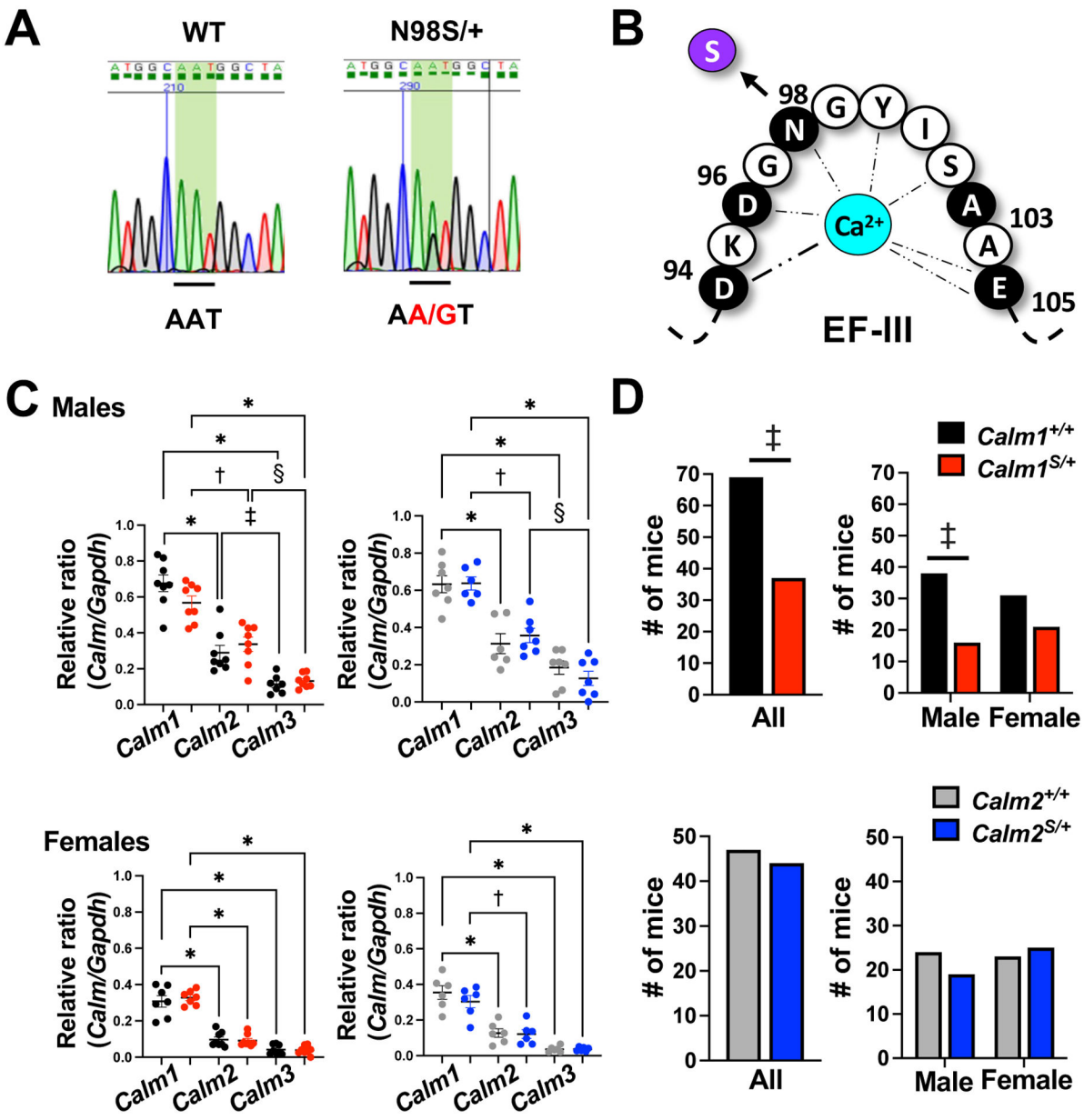

Figure 1.

Calmodulin gene expression and birth ratios in N98S knock-in mice. Heterozygous N98S (S/+) knock-in C57BL/6J mice were engineered using CRISPR/Cas9 genome editing. (**A**) Sanger sequencing showing asparagine-98 (N98) modified to serine (S) with a single nucleotide change of codon 98 (c.293A>G; N98S). (**B**) A schematic showing the location of the N98S mutation within the third EF-hand of the CaM C-domain. The dashed lines indicate Ca^{2+} chelating positions. Codon numbers are indicated along with single letter amino acid codes. (**C**) Quantitative RT-ddPCR was performed and the expression levels of the three calmodulin genes were assessed in male (top) and female (bottom) hearts from *Calm1* (left) or *Calm2* (right) S/+ and wild type (+/+) littermate mice. Data from $Calm1^{S/+}$ mice are displayed as red dots, with $Calm1^{+/+}$ littermate mice displayed as black dots. Data

from *Calm2*$^{S/+}$ mice are displayed as blue dots, with *Calm2*$^{+/+}$ littermate mice displayed as gray dots. Data are displayed as scatter dot plots with lines representing the mean and SEM. One-way ANOVA was used to compare gene expression of the same sex and two-way ANOVA was used to compare gene expression between male and female mice. Number of replicates are provided in Supplemental Table S4. (**D**) Genotypes of mice were quantified in each group to assess birth ratios for all mice (left) or separately for male and female mice (right). Chi-square analysis was used for birth ratios. Significance levels are denoted by * for $p<0.0001$, † for $p<0.001$, ‡ for $p<0.05$, § for $p<0.01$.

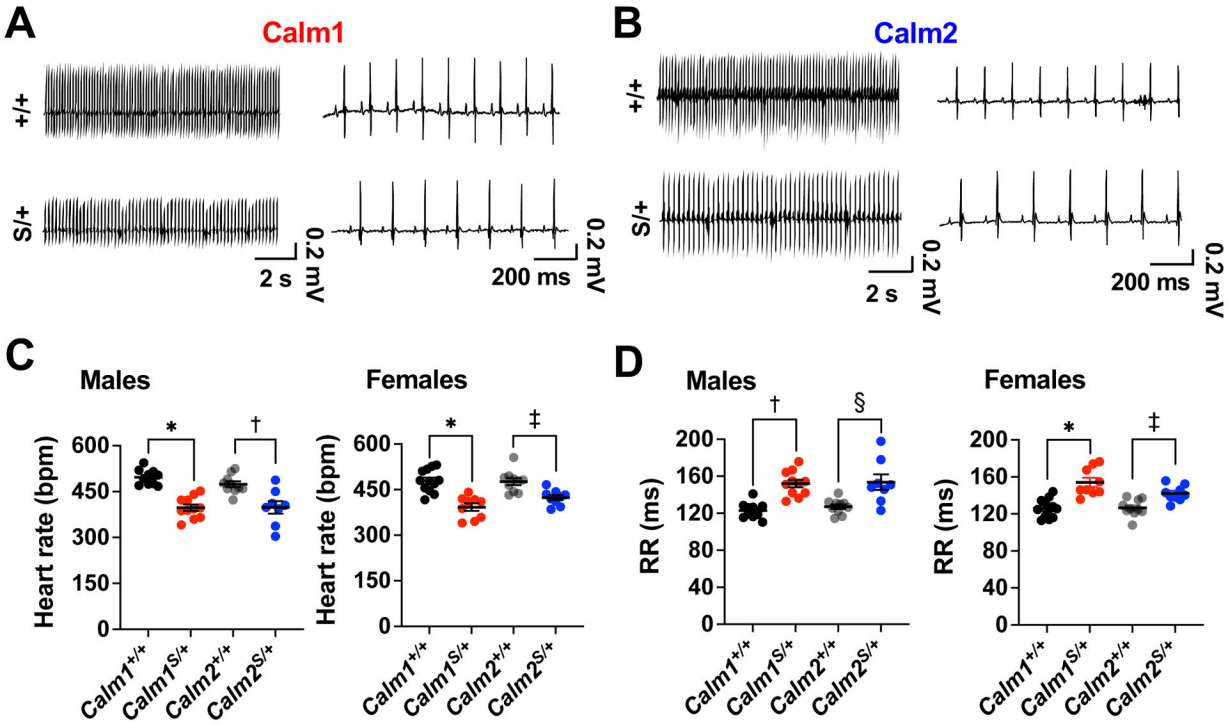

Figure 2.

Calm1$^{S/+}$ and *Calm2*$^{S/+}$ mice have bradycardia. Surface ECG recordings were performed in anesthetized 2 to 4-month-old mice. (**A**) Representative baseline ECG traces of *Calm1*$^{+/+}$ (top) and mutant *Calm1*$^{S/+}$ (bottom) mice. (**B**) Representative baseline ECG traces of *Calm2*$^{+/+}$ (top) and mutant *Calm2*$^{S/+}$ (bottom) mice. (**C**) Baseline heart rates of *Calm1*$^{+/+}$ and *Calm1*$^{S/+}$ or *Calm2*$^{+/+}$ and *Calm2*$^{S/+}$ male (left) and female (right) mice. (**D**) Baseline RR-intervals for *Calm1*$^{+/+}$ and *Calm1*$^{S/+}$ or *Calm2*$^{+/+}$ and *Calm2*$^{S/+}$ male (left) and female (right) mice. Data are displayed as scatter plots (*Calm1*$^{+/+}$, black; *Calm2*$^{+/+}$, gray; *Calm1*$^{S/+}$, red; *Calm2*$^{S/+}$, blue) with horizontal lines representing the mean ± SEM. Number of replicates are provided in Supplemental Table S7. Data were analyzed using a one-way ANOVA. Significance levels are denoted by * for $p<0.0001$, † for $p<0.001$, ‡ for $p<0.05$, § for $p<0.01$.

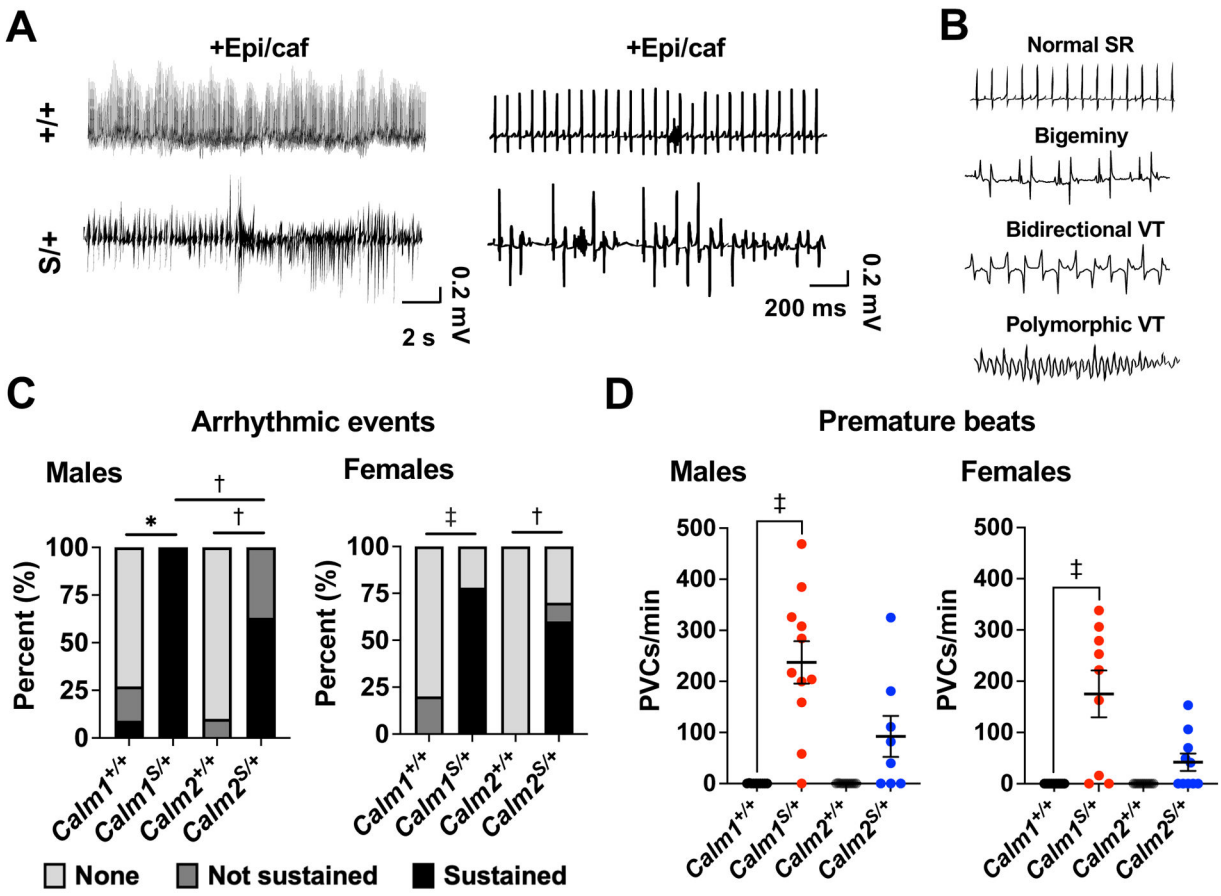

Figure 3.

Heterogeneity of arrhythmia phenotypes in *Calm1*$^{S/+}$ and *Calm2*$^{S/+}$ mice. Surface ECG recordings were performed in anesthetized 2 to 4-month-old mice. After baseline recording, epinephrine (2 mg/kg) and caffeine (120 mg/kg) were administered by intraperitoneal (i.p.) injection. (**A**) Example ECG traces recorded from *Calm1*$^{+/+}$ (top) and male *Calm1*$^{S/+}$ (bottom) mice after administration of epinephrine and caffeine (epi/caf). (**B**) Examples of the different observed arrhythmic events. (**C**) Data showing the percentage of mice with arrhythmic events observed after epi/caf administration. Data were analyzed using Fisher's exact test. Significance levels are denoted by * for $p<0.0001$, † for $p<0.05$, ‡ for $p<0.001$. (**D**) Quantification of premature beats after epi/caf administration in male (left) and female (right) groups of *Calm1*$^{+/+}$ (black symbols), *Calm1*$^{S/+}$ (red symbols), *Calm2*$^{+/+}$ (gray symbols) and *Calm2*$^{S/+}$ (blue symbols) mice. Premature beats were quantified as the average number of PVCs/minute of three 1-minute time periods at 4, 8, and 12 minutes after epi/caf. Horizontal lines represent mean ± SEM. Number of replicates are provided in Supplemental Table S8. Data were analyzed using a Kruskal-Wallis test. Significance levels are denoted by * for $p<0.0001$, † for $p<0.05$, ‡ for $p<0.001$.

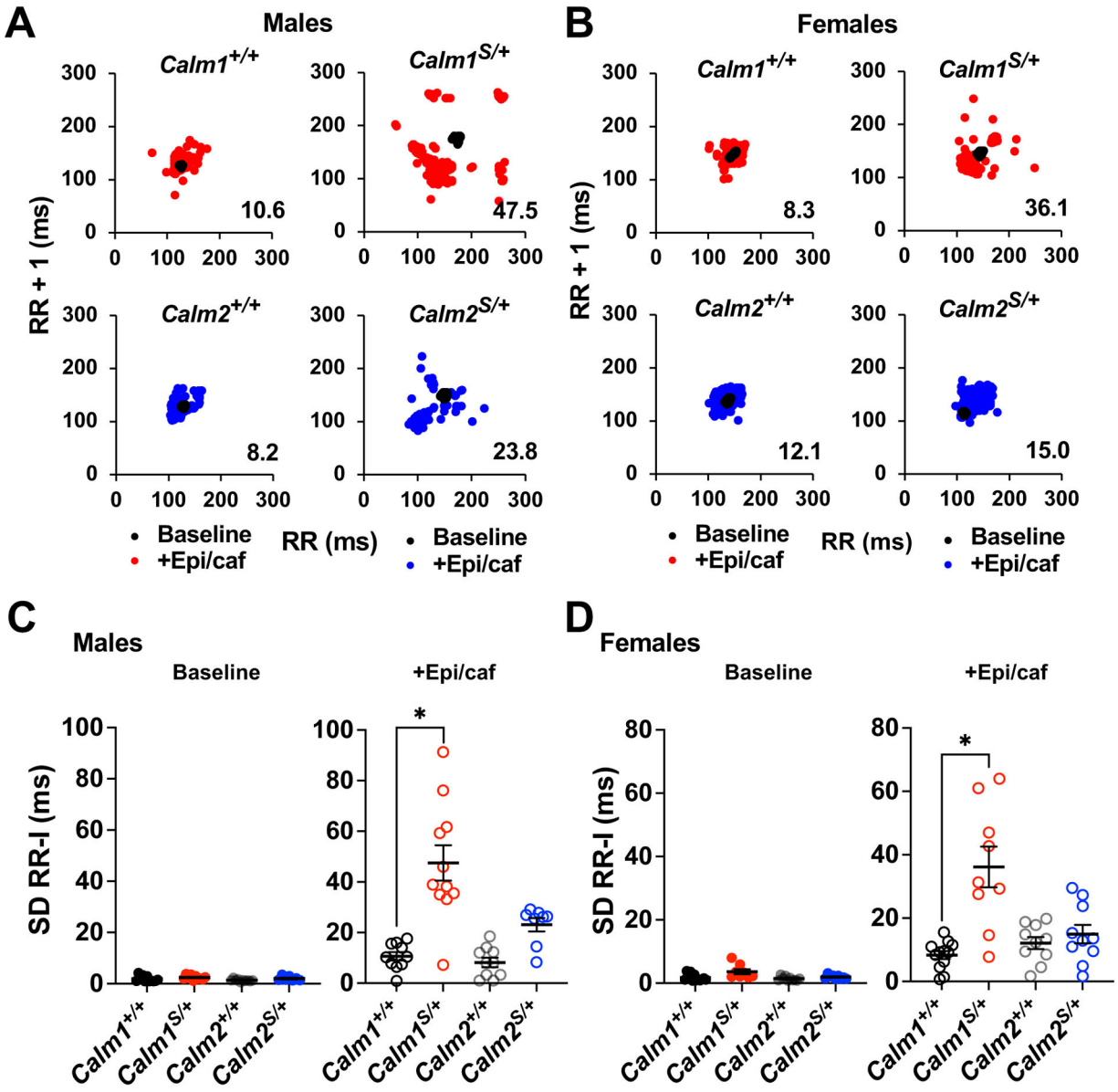

Figure 4.

Heart rate variability in WT, *Calm1*$^{S/+}$ and *Calm2*$^{S/+}$ mice. Surface ECG recordings were performed in anesthetized 2 to 4-month-old mice before and after epi/caf administration. Representative Poincaré plots showing the RR interval (RR-I) vs the RR-I of the next beat (RR-I+1) at baseline (black dots) and 10 minutes after epi/caf (red dots, *Calm1;* blue dots, *Calm2*) in (**A**) male and (**B**) female mice. (**C,D**) Quantification of heart rate variability presented as the standard deviation of the RR interval at baseline (solid data symbols) and after epi/caf administration (open data symbols) in male (**C**) and female (**D**) mice. Horizontal lines represent mean ± SEM. Number of replicates are provided in Supplemental Table S10. Data were analyzed using a Kruskal-Wallis test. Significance levels are denoted by * for $p<0.001$.

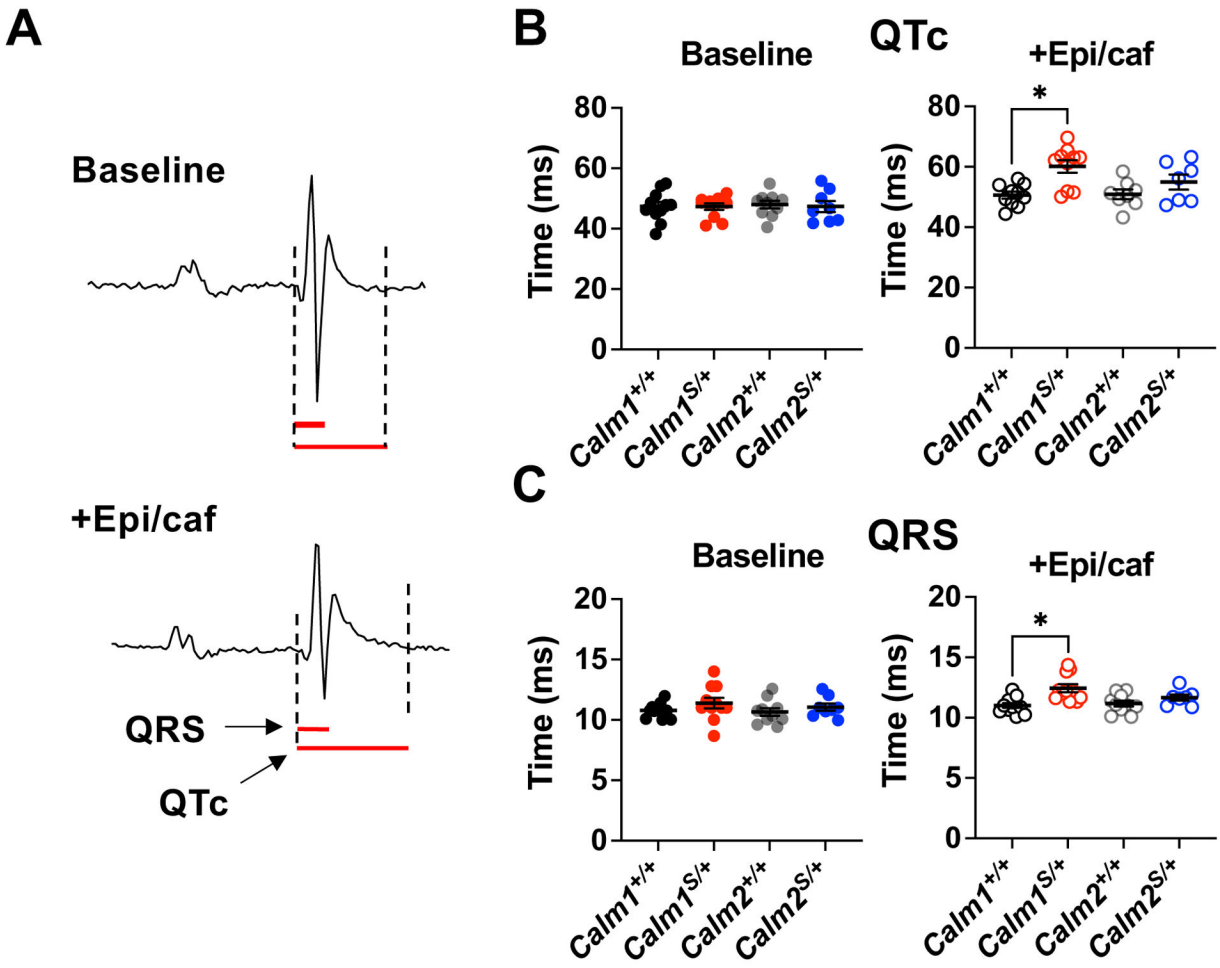

Figure 5.

Epinephrine/caffeine prolongs QTc and QRS in male *Calm1*$^{S/+}$ mice. epi/caf administration. (**A**) A representative single beat ECG trace recorded from a male *Calm1*$^{S/+}$ mouse at baseline (top) and after epi/caf administration (bottom). (**B**) Average QTc interval measured in male *Calm1*$^{S/+}$ and *Calm2*$^{S/+}$ mice at baseline (left) and after epi/caf (right). (**C**) Average QRS duration measured in male *Calm1*$^{S/+}$ and *Calm2*$^{S/+}$ mice at baseline (left) and after epi/caf (right). Horizontal lines represent mean ± SEM. Number of replicates are provided in Supplemental Table S7. Data were analyzed using a one-way ANOVA. Significance levels are denoted by * for $p<0.01$.

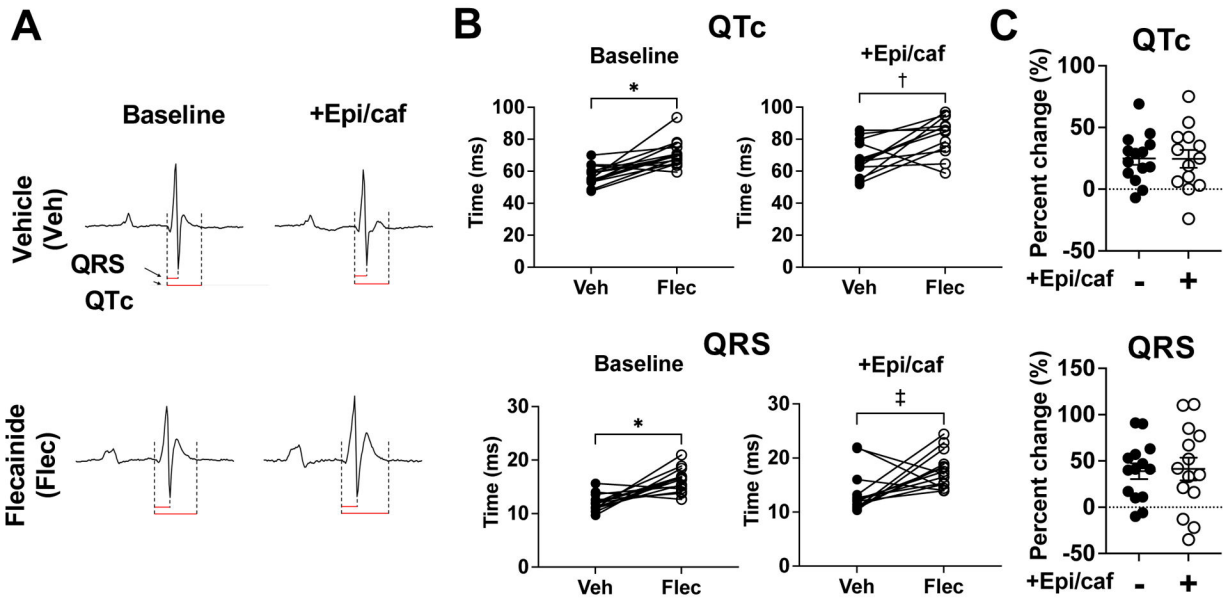

Figure 6.

Flecainide prolongs the QTc interval and QRS duration in N98S mice. Surface ECG recordings were performed on anesthetized 2 to 4-month-old mice. Flecainide (Flec, 20 mg/kg) or vehicle (Veh, DMSO:PBS) was administered by intraperitoneal (i.p.) injection 30 minutes before administration of epinephrine (epi, 2 mg/kg, i.p.) and caffeine (caf, 120 mg/kg, i.p.). (**A**) Representative PQRST complexes recorded from a female N98S mouse that received a vehicle (top) injection, with the procedure repeated 7 days later with a flecainide (bottom) injection. Example traces obtained at baseline and following epi/caf administration. (**B**) Changes in QTc and QRS duration of female N98S mice following flecainide or vehicle administration with or without epi/caf exposure. Pairs of connected symbols represent individual mice. (**C**) Percent difference in QTc and QRS duration between vehicle and flecainide treated mice. Number of replicates are provided in Supplemental Table S12. Data were analyzed using a Student's t-test. Significance levels are denoted by * for $p<0.001$, † for $p<0.01$, ‡ for $p<0.05$.

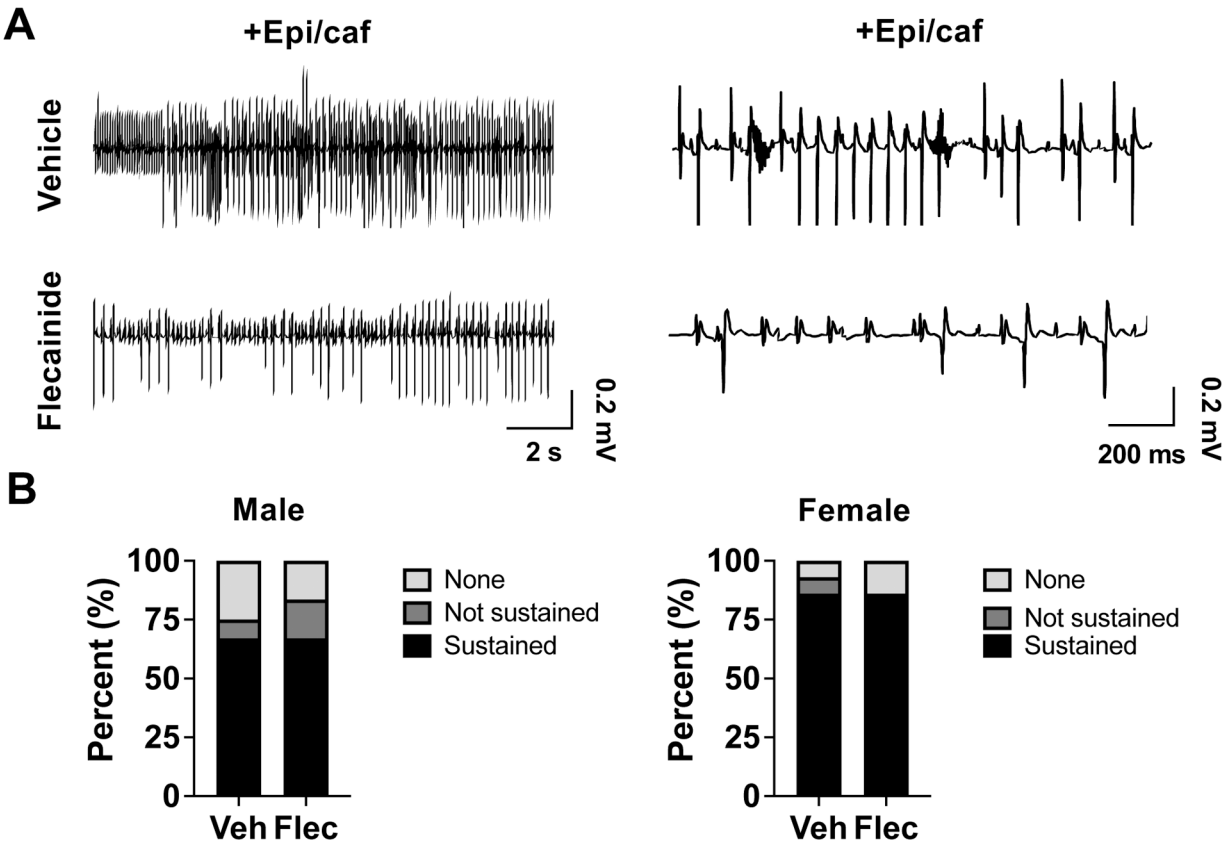

Figure 7.

Flecainide does not prevent arrhythmia in N98S mice. Surface ECG recordings were performed on anesthetized 2 to 4-month-old *Calm1*$^{S/+}$ and *Calm2*$^{S/+}$ mice. Flecainide (Flec, 20 mg/kg) or vehicle (Veh) was administered by intraperitoneal (i.p.) injection 30 minutes before administration of epinephrine (epi, 2 mg/kg, i.p.) and caffeine (caf, 120 mg/kg, i.p.). Experiments were repeated 7 days later with mice being placed in the other treatment group. (**A**) Representative ECG traces recorded after epi/caf from a female *Calm2*$^{S/+}$mouse pre-treated with vehicle or flecainide. (**B**) Percentage of mice with sustained, not sustained or no arrhythmic events observed after epi/caf administration in vehicle or flecainide pre-treated male *(*n=12*, left)* and female *(*n=14, *right)* mice. Number of replicates are provided in Supplemental Table S13. Data were analyzed using a Fisher's exact test. There were no significant differences between vehicle-treated and flecainide-treated groups.

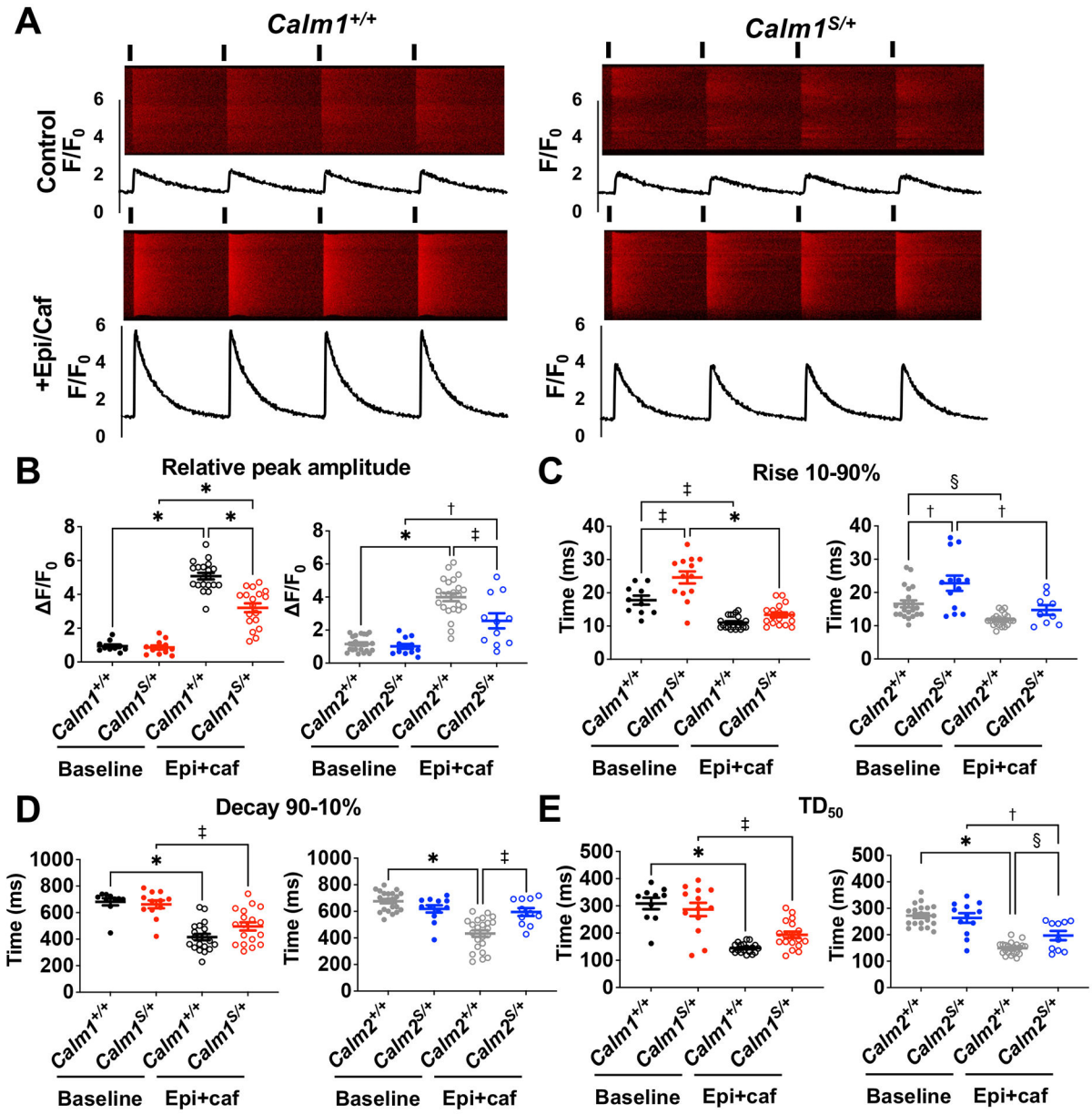

Figure 8.

Ca^{2+} transients in cardiomyocytes from male *Calm1*$^{S/+}$ and *Calm2*$^{S/+}$ mice. Intracellular Ca^{2+} transients were imaged in single ventricular cardiomyocytes using line scan fluorescence detection on a confocal microscope. (**A**) Representative transients from male WT *Calm1*$^{+/+}$ (left) and mutant *Calm1*$^{S/+}$ (right) cardiomyocytes paced at 1 Hz (cycle length 1000 ms) in 1 mM [Ca^{2+}] normal Tyrode's solution (top) or with 1 mM [Ca^{2+}] Tyrode's solution with 10 μM of epinephrine and 250 μM of caffeine. (**B**) Peak Ca^{2+} transient amplitudes determined as the change in fluorescence from initiation of Ca^{2+} rise to peak Ca^{2+} (ΔF) normalized to the fluorescence at baseline (F_0). (**C**) Rise time of Ca^{2+} transients. (**D**) Decay time of Ca^{2+} transients. (**E**) Duration of Ca^{2+} transients at 50% recovery (TD_{50}). Data in B-E are scatter plots with lines representing the mean and the SEM. Filled symbols

represent data collected in 1 mM [Ca^{2+}] normal Tyrode's solution while open symbols represent data collected in 1 mM [Ca^{2+}] Tyrode's solution with 10 μM of epinephrine and 250 μM of caffeine. Data are from 10–20 cells from 3–4 mouse hearts in each genotype group. Numeric data for 1Hz and 3.3Hz pacing are provided in Supplemental Tables S14–S17. Data were analyzed using a one-way ANOVA. Significance levels are denoted by * for $p<0.0001$, † for $p<0.01$, ‡ for $p<0.001$, and § for $p < 0.05$.

Table 1.

Clinical features of reported patients with the N98S variant.

Gene	Sex	Age at diagnosis	Clinical presentation	ECG features	QTc (ms)	Treatment	Reference
CALM1	F	4 years	SCA, syncope	ventricular ectopy, BVT	not prolonged	β-blocker, ICD	4
CALM1	M	5 years	SCA	VF	494	nd	23
CALM2	M	5 years	syncope, seizure	biphasic T wave	478 at baseline; 558 after epi	β-blocker, mexiletine	6
CALM2	M	7 years	SCD	sinus bradycardia, bigeminy, polymorphic PVCs, biphasic T wave	432	none	22
CALM2	F	4 years	VF	SCA, VF	412 at baseline; 528 after epi	β-blocker, ICD	22
CALM2	M	4 years	VF, TdP	SCA, VF, PVT, TdP, biphasic T wave	635	β-blocker	24

SCA, sudden cardiac arrest; SCD, sudden cardiac death; ICD, implantable cardioverter defibrillator; PVC, premature ventricular contraction; BVT, bidirectional ventricular tachycardia; TdP, torsades de pointes; epi, epinephrine infusion test; VF, ventricular fibrillation; nd, not described.

Table 2.

Comparison of CPVT and calmodulinopathy mouse models.

CPVT						
Mutation	**Mouse strain**	**Phenotype**	**β-AR induced**	**Cellular Ca^{2+} dynamics**	**Response to flecainide**	**Reference**
Casq2 $^{-/-}$	C57BL/6	↓HR, bigeminy, BVT, PVT	Yes	↑spontaneous premature Ca^{2+} release, SR Ca^{2+} leak	↓ arrhythmias	30, 43
RyR2 $^{R4496C/+}$	C57BL/6	BVT, VF, VT	Yes	↑spontaneous premature Ca^{2+} release	↓ arrhythmias	26, 32
RyR2 $^{R176Q/+}$	C57BL/6	BVT	Yes	↑spontaneous premature Ca^{2+} release	Not tested	42
Calmodulinopathy						
Calm1 $^{N98S/+}$	C3HeB/FeJ x C57BL/6J	↓HR, bigeminy, BVT, PVT, LQT	Yes	no spontaneous premature Ca^{2+} release, ↓resting spark frequency, ↓spark amplitude	Not tested	41
Calm1 $^{N98S/+}$	C57BL/6J	↓HR, bigeminy, BVT, PVT, LQT (males)	Yes	no spontaneous premature Ca^{2+} release, ↓peak amplitude	ineffective	*This study*
Calm2 $^{N98S/+}$	C57BL/6J	↓HR, bigeminy, BVT, PVT	Yes	no spontaneous premature Ca^{2+} release, ↓peak amplitude	ineffective	*This study*

HR, heart rate; VT, ventricular tachycardia; BVT, bidirectional VT; PVT, polymorphic VT; VF, ventricular fibrillation; LQT, long-QT; ↑ = greater; ↓ = fewer